NP-1250, an ABCG2 inhibitor, induces apoptotic cell death in mitoxantrone-resistant breast carcinoma MCF7 cells via a caspase-independent pathway

MASUMI ITO[1,2], KAZUNORI KAJINO[1], MASAAKI ABE[1], TSUTOMU FUJIMURA[3], REIKO MINEKI[3], TAKAKO IKEGAMI[4], TOSHIHISA ISHIKAWA[5] and OKIO HINO[1]

[1]Department of Pathology and Oncology, Juntendo University School of Medicine, Bunkyo, Tokyo 113-8421; [2]Nippon Chemiphar Co., Ltd., Saitama 341-0005; [3]Laboratory of Proteomics and Biomolecular Science, Biomedical Research Center, Juntendo University Graduate School of Medicine, Bunkyo, Tokyo 113-8421; [4]Laboratory of Molecular and Biochemical Research, Research Support Center, Juntendo University Graduate School of Medicine, Bunkyo, Tokyo 113-8421; [5]Omics Science Center, RIKEN Yokohama Institute, Yokohama 230-0045, Japan

Received September 10, 2012; Accepted November 9, 2012

DOI: 10.3892/or.2013.2249

Abstract. Chemoresistance is one of the main obstacles to successful cancer therapy and is frequently associated with multidrug resistance (MDR). One of the most studied mechanisms of MDR is the high expression of ATP-binding cassette (ABC) transporters. Here, we demonstrated that NP-1250, an ABCG2 inhibitor, induced apoptotic cell death in ABCG2-overexpressing multidrug-resistant MCF7/mitoxantrone-resistant (MX) human breast carcinoma cells via a caspase-independent pathway. Incubation of MCF7/MX cells with NP-1250 significantly reduced cell viability, while NP-1250 had little effect on the viability of drug-sensitive MCF7/wild-type cells. Although the target molecules of NP-1250 in cell death remain unknown, investigation of NP-1250 will aid in the elucidation of the molecular mechanism of drug resistance and NP-1250 may become a new therapy for MDR cancers.

Correspondence to: Dr Okio Hino, Department of Pathology and Oncology, Juntendo University School of Medicine, 2-1-1 Hongo, Bunkyo, Tokyo 113-8421, Japan
E-mail: ohino@juntendo.ac.jp

Abbreviations: ABC, ATP-binding cassette; Flp-In-293/ABCG2 cells, ABCG2-overexpressing Flp-In-293 cells; Flp-In-293/Mock cells, mock-transfected Flp-In-293 cells; MCF7/MX cells, mitoxantrone-resistant MCF7 cells; MCF7/WT cells, wild-type MCF7 cells; MDR, multidrug resistance; MTX, methotrexate; PARP, poly(ADP-ribose) polymerase; PDIA4, protein disulfide-isomerase A4; PHB2, prohibitin-2; PRDX2, peroxiredoxin-2

Key words: breast cancer, mitoxantrone resistance, caspase-independent cell death, ABCG2, apoptosis

Introduction

A frequent problem in cancer chemotherapy is the development of multidrug resistance (MDR) which renders tumors unresponsive to a diverse array of compounds. There are a number of mechanisms by which a cell can acquire MDR, one of the most common being overexpression of members of the ATP-binding cassette (ABC) transporter family. This is a group of plasma membrane proteins that actively extrude a broad range of substrates from cells. They are predominantly found in areas such as the epithelial cells of the intestine, hepatocytes, capillary epithelial cells of the blood-brain barrier, and in various stem cells where the physiological role of these ATPase efflux 'pumps' is to protect cells from damage by rapidly extruding xenobiotics (1). Unfortunately, their unwanted expression in tumor cells can lead to chemotherapy resistance in these cells (2).

Most research concerning ABC transporter-overexpressing MDR cancer cells have focused on molecules or signaling pathways that regulate expression of these transporters (3,4), and a few potential therapeutic target molecules have been identified. In recent years, it has been reported that suppression of ABC transporters inhibits cancer cell proliferation, particularly in transporter-overexpressing MDR cancer cells (5,6). However, there are no reports concerning the relationship between inhibition of ABC transporters and cell death.

In the present study, we demonstrated that treatment with NP-1250, an ABCG2 inhibitor, alone induced apoptotic cell death via a caspase-independent pathway in MDR MCF7 breast cancer cells (MCF7/MX). MCF7/MX cells (1) have the MDR phenotype characterized by high levels of the ABCG2 transporter. We speculated that NP-1250 would have an effect on molecules involved in growth and survival, whose expression levels have been elevated in the process of acquiring resistance to anticancer drugs. Using a proteomics approach, we identified three candidate molecules: peroxiredoxin-2,

protein disulfide-isomerase A4 and prohibitin-2. These molecules may be potential candidates for the treatment of MDR cancers.

Materials and methods

Materials. Pan-caspase inhibitor (Z-VAD-FMK) and caspase-3/7-specific inhibitor (Ac-DEVD-CHO) were purchased from Promega (Madison, WI, USA). Doxorubicin was obtained from Kyowa Hakko Kirin (Tokyo, Japan) and mitoxantrone hydrochloride was obtained from Wyeth Lederle Japan, Ltd. (Tokyo, Japan). NP-1250 was synthesized at Nippon Chemiphar Co., Ltd. (Saitama, Japan). It is still under development, therefore, disclosure of the structure of this compound is prohibited.

Cell cultures and treatment. The MCF7 human breast cancer cell line, the HL-60 human promyelocytic leukemia cell line, the multidrug-resistant HL-60/MX1 cell line, the MES-SA human uterus sarcoma cell line, and the multidrug-resistant MES-SA/Mx2 and MES-SA/Dx5 cancer cell lines were obtained from American Type Culture Collection (ATCC, Rockville, MD, USA) and cultured in the recommended medium containing 10% heat-inactivated fetal bovine serum (FBS) at 37˚C in a 95% air/5% CO_2 atmosphere. Mitoxantrone-resistant MCF7 (MCF7/MX) cells (7) were a gift from Dr Masayuki Nakagawa (Department of Urology, Kagoshima University, Kagoshima, Japan) and doxorubicin-resistant MCF7 (MCF7/DOX) cells were a gift from Dr Takao Yamori (Division of Molecular Pharmacology, Cancer Chemotherapy Center, Japanese Foundation for Cancer Research, Tokyo, Japan). Prior to any experiments, MCF7/MX cells and MCF7/DOX cells were maintained in drug-free medium for one passage. Other resistant cells were cultured in the absence of anticancer drugs. ABCG2-overexpressing Flp-In-293 (Flp-In-293/ABCG2) cells and mock-transfected Flp-In-293 (Flp-In-293/Mock) cells were established and cultured as previously described (8).

Evaluation of the inhibitory effect on the ABCG2 transporter. To evaluate ABCG2-NP-1250 interaction, plasma membrane vesicles prepared from ABCG2-expressing Sf9 cells were incubated with [^{3}H]methotrexate (MTX). Transport into the vesicles was measured by counting the radioactivity remaining on the filter of MultiScreen plates, as previously described (9).

Cell viability assay. To evaluate the effectiveness of NP-1250 in overcoming ABCG2-mediated drug resistance, Flp-In-293/ABCG2 and MCF7/MX cells were incubated with anticancer drug SN-38 and NP-1250, and the cell viabilities were measured.

Tumor cells were seeded in 96-well plates. After 24 h, the medium was replaced with medium containing different concentrations of NP-1250 in triplicate. After a 72-h incubation at 37˚C, cell viability was determined at the indicated times, as previously described (10).

TUNEL staining. MCF7/WT and MCF7/MX cells were seeded in 35-mm glass-bottom dishes. After 24 h, the medium was replaced with medium containing 10, 20 or 40 μM of NP-1250. After a 48-h incubation at 37˚C, TUNEL staining was performed as previously described (10). The frequency (%) of TUNEL-positive cells per DAPI-positive cells was determined in five different fields in duplicate. Two replicate experiments were performed.

Annexin V/PI staining. The Annexin V-FITC fluorescence microscopy kit (Pharmingen, San Diego, CA, USA) was used to detect apoptosis. MCF7/MX cells were seeded in 35-mm glass-bottom dishes. After 6, 12, 24 or 48 h of incubation with 20 μM of NP-1250 at 37˚C, Annexin V/propidium iodide (PI) staining was performed according to the manufacturer's protocol. Stained cells were visualized using a confocal microscope (Leica).

RNA isolation and cDNA synthesis. Total RNA was prepared using the FastPure® RNA kit (9190; Takara, Shiga, Japan) according to the manufacturer's protocol, and RNA concentrations were measured at an absorbance A_{260}. Reverse transcription (RT) was carried out with 1 μg RNA using a ReverTraAce® qPCR RT kit (FSQ-101; Toyobo, Osaka, Japan).

Real-time PCR. Real-time PCR was carried out using Fast SYBR-Green Master Mix (4385612, Applied Biosystems, Life Technologies Corp., Carlsbad, CA, USA) using a 7500 Fast Real-Time PCR system (Applied Biosystems). All primers used for real-time PCR are described in Table I. PCR was carried out with an initial 20-sec denaturation at 95˚C followed by 40 cycles of PCR (3 sec at 95˚C and 30 sec at 60˚C). Reactions were performed in triplicate for three biological replicates, and the amount of each cDNA was normalized to GAPDH gene expression. Melt-curve analysis was performed to ensure that the mRNA-specific fragments were amplified and data were analyzed using the standard curve method.

Immunofluorescence staining of ABCG2. Cells were fixed in 4% paraformaldehyde, permeabilized with 0.2% Triton X-100, and blocked with 1% bovine serum albumin and 10% normal goat serum in phosphate-buffered saline (PBS). Incubation with primary monoclonal antibody for ABCG2 (ALX-801-029; Wako, Osaka, Japan) at a dilution of 1:200 was carried out overnight at 4˚C, followed by incubation with the Alexa Fluor-conjugated secondary antibody (A11001; Molecular Probes, Inc., Carlsbad, CA, USA) for 1 h at room temperature. Immunofluorescence was detected and analyzed using a Leica TCS SP5 Laser Scanning Confocal Microscope system.

Western blot analysis. Cells were washed two times with PBS, harvested by scraping from the culture dishes in lysis buffer and collected. Protein concentrations were determined using the DC protein assay kit according to the manufacturer's instructions (500-0116; Bio-Rad, Hercules, CA, USA). Equal amounts of proteins were denatured by boiling and subjected to SDS-polyacrylamide gel electrophoresis. The separated proteins were transferred to polyvinylidene difluoride membranes. The membranes were incubated overnight at 4˚C with primary polyclonal antibody at a dilution of 1:1000 for caspase-3, cleaved-PARP, cleaved-caspase-7 or cleaved-caspase-9 (9665, 9541, 9491, 9501; Cell Signaling Technology,

Table I. Sequence of primers for real-time PCR.

Gene	Direction	Primer sequence (5'-3')	Product size (bp)
GAPDH	Forward	GCCATCAATGACCCCTTC	114
	Reverse	GATGACAAGCTTCCCGTTC	
ABCB1	Forward	AACTTCCGAACCGTTGTTTC	110
	Reverse	CCAAAGATGTGTGCTTTCCTC	
ABCC1	Forward	CTACCTCCTGTGGCTGAATC	150
	Reverse	ATCAGCTTGATCCGATTGTC	
ABCG2	Forward	ACAGGTGGAGGCAAATCTTC	94
	Reverse	GCGGTGCTCCATTTATCAG	
PRDX1	Forward	CTGTCATCTAGCATGGGTCAAT	106
	Reverse	CCCATAATCCTGAGCAATG	
PRDX2	Forward	GTCCGTGCGTCTAGCCTTTG	128
	Reverse	CAGCTTCACCTCTTTGAAGG	
LGUL	Forward	CCAAGGATTTTCTATTGCAG	97
	Reverse	TGGATTAGCGTCATTCCAAGA	
GLTP	Forward	CCCTTCTTCGATTGCCTTG	107
	Reverse	AACTTGGCTGGGTTGGTGTC	
TAGL2	Forward	CCAAACTGTGGACCTCTGG	143
	Reverse	GATTCTCCTTGGATTTCTTAGGG	
PSB5	Forward	CCACCCTGGCCTTCAAGTTC	132
	Reverse	CCATGGTGCCTAGCAGGTATG	
PEBP1	Forward	GCCCACCCAGGTTAAGAATAG	145
	Reverse	GACCACCAGGAAATGATGC	
GNA1	Forward	CCTGTGCTAAGAGAGGAAGAGT	143
	Reverse	TGGTAGACATTCAAGGGTAATC	
DCTP1	Forward	CTTTCAGTGGAAAACCGATG	144
	Reverse	ACTGCTAGCGGCAGATCCAC	
VDAC2	Forward	GATTTGGTTTTGGGTTGGTG	115
	Reverse	TCCAAGGTCCCAGTAACTTT	
P5CR1	Forward	TGGACCTGGCCACAGTTT	103
	Reverse	TTCACAGCCAGGAAGAGCACAT	
SFXN1	Forward	TTGGCTTCTGTTTGGTGTTT	113
	Reverse	GCTCTCTTGGATCTTAGCTTGC	
PDIA4	Forward	CCGCTAACAACCTGAGAGAAG	105
	Reverse	CAGGCTGCATTACAACCAAC	
HNRPM	Forward	AAGGGTGAAGGAGAACGACCTG	111
	Reverse	GGCTCTGTATCTTTTAGTTGGA	
ECHA	Forward	AACTCTCCCAATTCAAAGGT	117
	Reverse	TGATGAGATAAGGACGGCACT	
GPDM	Forward	TCACCAGAGGACTAAAAACAGC	91
	Reverse	ACACCACCATGGATCAATTT	
IPYR	Forward	AATGGAGATTGCTACAAAGGAC	142
	Reverse	TGGGTCTTCCCAAGTCTG	
OTUB1	Forward	CAGCGGTTCAAGGCTGTGT	133
	Reverse	CGACAGAGGTCTGCTTCTCC	
PHB2	Forward	CTCCAAAGACCTACAGATGGTG	130
	Reverse	GTTGACAATGGACGGCAACA	
GGCT	Forward	CCGCCTGCAGGATTTTAAG	98
	Reverse	CGCCAGGACTCTGAAAAATG	
LDHA	Forward	CTGTCATGGGTGGGTCCTT	106
	Reverse	CCCTAAATCTGGGTGCAGAGTC	

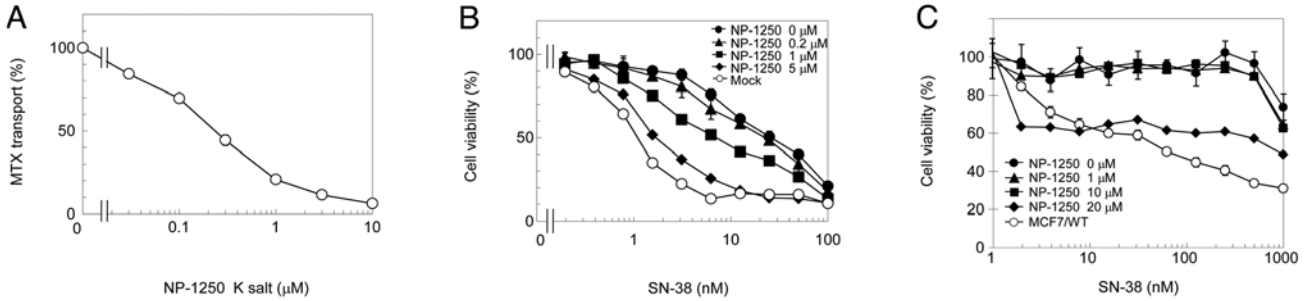

Figure 1. Inhibitory effect of NP-1250 on the ABCG2 transporter. (A) Inhibition of ABCG2-mediated [^{3}H]MTX transport by NP-1250. MTX transport is expressed as relative values compared with the transport activity measured without NP-1250 (100% MTX transport). Data points, means; bars, SD (n=4). (B and C) Reversal of ABCG2-mediated SN-38 resistance by NP-1250. NP-1250 dose-dependently reversed SN-38 resistance in Flp-In-293/ABCG2 cells (B) but had no similar effect in MCF7/MX cells (C). However, in MCF7MX cells (C), 20 μM of NP-1250 inhibited cell viability with a very low dose of SN-38. Data points, means; bars, SD (n=4).

Beverly, MA, USA). Membranes were then incubated with goat anti-rabbit IgG-HRP secondary antibody for 1 h at room temperature and visualized using an enhanced chemiluminescence detection system.

Proteomics

SDS-PAGE and detection by MS compatible silver staining. MCF7/WT and MCF7/MX cells were fractionated using the ProteoExtract® Subcellular Proteome Extraction kit (Merck KGaA, Darmstadt, Germany). Protein samples (5 μg) were separated by SDS-PAGE. Upon completion, the gel was transferred to a clean and dry glass chamber for silver staining using the PlusOne Silver Staining kit, Protein (GE Healthcare, Hino, Japan).

Identification of protein. In-gel digestion using trypsin was performed as previously described (11). The tryptic peptides were used for identification of proteins by mass spectrometry. The digested peptides were analyzed using a nanoflow LC-MS/MS system with a direct nanoflow LC system (DiNa; KYA Technologies, Tokyo, Japan) and a LTQ Orbitrap XL-ETD mass spectrometer (Thermo Fisher Scientific, Inc., Waltham, MA, USA). Data were searched against NCBI human sequence database using Mascot (Matrix Science, Ltd., London, UK).

Statistical analysis. The results are expressed as means ± SD. Each value represents the mean ± SD of two or three independent experiments. One-way analysis of variance (ANOVA) with Dunnett multiple comparison test and t-test were performed, and $P<0.01$ was considered to indicate a statistically significant difference.

Results and Discussion

NP-1250 is an ABCG2 inhibitor and treatment alone reduces the cell viability of ABCG2-overexpressing MCF7/MX cells. We measured ATP-dependent [^{3}H]MTX transport in plasma membrane vesicles, prepared from ABCG2-expressing Sf9 cells, in the presence of a potassium salt of NP-1250. Potassium salt of NP-1250 inhibited ABCG2-mediated MTX transport in a dose-dependent manner (Fig. 1A). This degree of inhibition was comparable to gefitinib (9), suggesting that NP-1250 is a powerful ABCG2 inhibitor. To examine whether NP-1250 overcomes ABCG2-mediated resistance, the cytotoxic effect of ABCG2-substrate SN-38 in the presence of NP-1250 on Flp-In-293/ABCG2 cells was measured. NP-1250 dose-dependently reversed SN-38 resistance in Flp-In-293/ABCG2 cells (Fig. 1B). We then evaluated NP-1250 on MCF7/MX cells, a mitoxantrone-resistant cell line in which ABCG2 was amplified and overexpressed (Fig. 2) by chronic exposure to mitoxantrone. Differing from our expectation, NP-1250 exhibited no reversing effect on MCF7/MX cells at concentrations <20 μM (Fig. 1C). Notably, 20 μM of NP-1250 inhibited cell viability with a very low dose of SN-38. These results suggest that ABCG2-inhibitor NP-1250 itself may have a cytotoxic effect.

NP-1250 induces apoptotic cell death in MCF7/MX cells. We compared the chemosensitivity to NP-1250 of drug-sensitive MCF7/WT cells and multidrug-resistant MCF7/MX cells by examining the cell viability and cell morphological changes. We discovered that NP-1250 alone reduced the cell viability of MCF7/MX cells, notably, more than that of MCF7/WT cells (Fig. 3A). For the cell morphological study, the number of MCF7/MX cells was significantly less than the number of cells in the control and the adherent cells displayed large vacuoles in the cytoplasm, exhibited atrophic changes or were almost dying (Fig. 3B). In contrast, little change was observed in MCF7/WT cells after a 72-h treatment (Fig. 3B). To confirm these initial observations, we analyzed apoptosis by TUNEL assay and phosphatidylserine (PS) externalization. After a 48-h treatment with NP-1250, in MCF7/MX cells, the number of TUNEL-positive cells was elevated (Fig. 3C) and the TUNEL-positive rate was significantly increased in a dose-dependent manner (Fig. 3D). Apoptotic cell death observed in the MCF7/MX cells upon treatment with NP-1250 was further confirmed by determining Annexin V binding to PS translocated from the inner to the outer membrane surface of the plasma membrane, a hallmark of early stage apoptosis (Fig. 3E).

NP-1250-induced cell death is 'caspase-independent apoptosis'. After 48 h of treatment with NP-1250, cleavage of PARP was detected using an antibody recognizing the 89-kDa fragment (Fig. 4A). Although PARP is a well-known substrate of

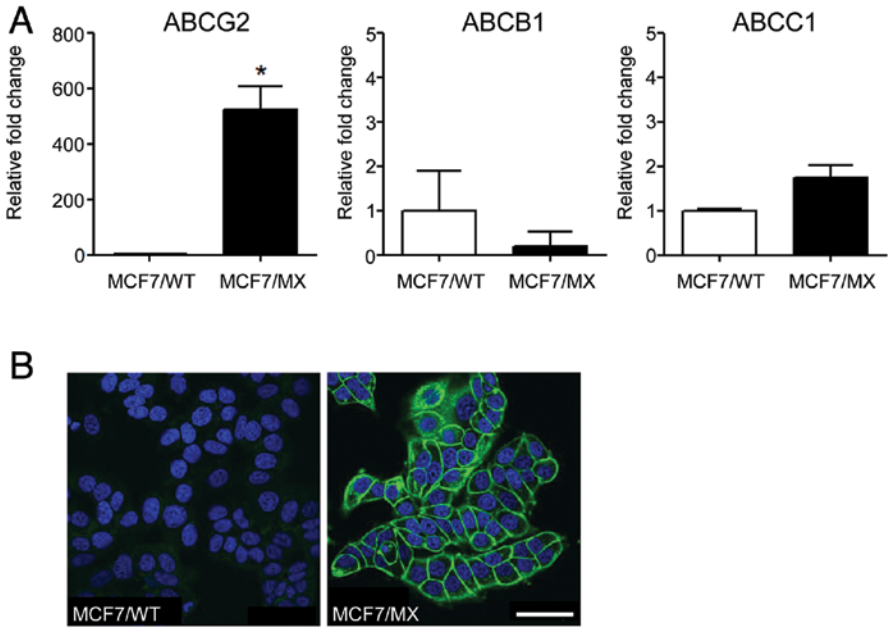

Figure 2. Expression of ABC transporters in human breast carcinoma MCF7/WT cells and multidrug-resistant MCF7/MX cells. (A) ABCG2, ABCB1 and ABCC1 mRNA expression as assessed by real-time PCR. MCF7/MX cells expressed a significantly increased level of ABCG2 mRNA (~500-fold) relative to MCF7/WT cells. Expression was normalized against the housekeeping gene GAPDH. Columns, means; bars, SD (n=3; *P<0.01). (B) Immunofluorescence of ABCG2. Highly expressed ABCG2 localized almost entirely at the cell membranes in MCF7/MX cells. Scale bar, 50 μm.

caspases, particularly caspase-3 and caspase-7, MCF7 cells do not express caspase-3 due to the deletion of 125 nucleotides in the CASP-3 mRNA (12). We confirmed the lack of caspase-3 protein in these MCF7/WT and MCF7/MX cells (data not shown). We, therefore, examined whether caspase-7 and caspase-9 were cleaved prior to cleavage of PARP, but we did not detect either one (Fig. 4A). To further ascertain whether NP-1250-induced apoptosis of MCF7/MX cells was caspase-dependent or -independent, MCF7/MX cells were pretreated with a caspase inhibitor prior to NP-1250 treatment, and cleavage of PARP was subsequently examined. Pretreatment with the pan-specific inhibitor completely abolished the cleavage of PARP, and the pharmacological inhibitor specific for caspase-3/7 also showed a significant inhibition of the cleavage of PARP (Fig. 4B). Under the same experimental conditions, pretreatment of MCF7/MX cells with these inhibitors did not block the production of apoptotic cells (Fig. 4C). These results suggest that caspases, which cleave PARP, are cleaved and activated upon exposure of MCF7/MX cells to NP-1250 but that this is not the main apoptotic cascade in the death of MCF7/MX cells.

To evaluate the effects of NP-1250 on other MDR cell lines that exhibit increased expression of ABC transporters, we treated several MDR cell lines and their drug-sensitive parental cell lines with NP-1250. We did not observe growth inhibition by NP-1250 in any of the cell lines (data not shown). We also treated several other cancer cell lines, specifically human hepatocellular carcinoma cell line HuH7, human cervical adenocarcinoma cell line HeLa and human mesothelioma cell lines H226 and MESO4, with NP-1250, but we did not confirm any effect (data not shown). Taken together, these results suggest that the antiproliferative/apoptotic effect of NP-1250 may be limited to MCF7/MX cells.

Search for target proteins by proteomics. There are no reports relating inhibition of ABC transporters to cell death, therefore, we speculated that NP-1250 may have other targets in MCF7/MX cells.

We excised several bands that were observed in the protein electrophoretograms of MCF7/MX cells. As a control, we also excised the band that appeared to be ABCG2, ~74 kDa, as observed in the membrane/organelle fraction of MCF7/MX cells. ABCG2 was identified in this band with a Mascot score of 192, thus we excluded proteins whose Mascot scores were <100. We also excluded proteins observed at positions >15 kDa different from their original molecular weight. Candidate proteins that passed our identification criteria are listed in Table II. We selected molecules preferentially involved in cell growth and survival from these proteins and performed real-time PCR to confirm whether the expression of genes encoding these proteins was increased in the MCF7/MX cells when compared to the MCF7/WT cells. Among the 46 proteins, we analyzed the gene expression of 22 proteins, including ABCG2. Three of these proteins, peroxiredoxin-2 (PRDX2), protein disulfide-isomerase A4 (PDIA4) and prohibitin-2 (PHB2), showed significantly elevated mRNA expression in MCF7/MX cells compared to the expression levels in MCF7/WT cells (Fig. 5). PDIA4 is a protein disulfide isomerase (PDI), an enzyme that catalyzes disulfide formation and isomerization and a chaperone that inhibits aggregation (13) and a member of a large family of dithiol/disulfide oxidoreductases, the thioredoxin superfamily. While it has been reported that PDI shows an inverse correlation with resistance (14), Liu *et al* reported that increased expression of PDI was found in multidrug-resistant MCF7/AdVp3000 cells when compared to MCF7 cells (15). PHB2, known as a repressor of estrogen receptor (ER) activity, has been shown to interact with and

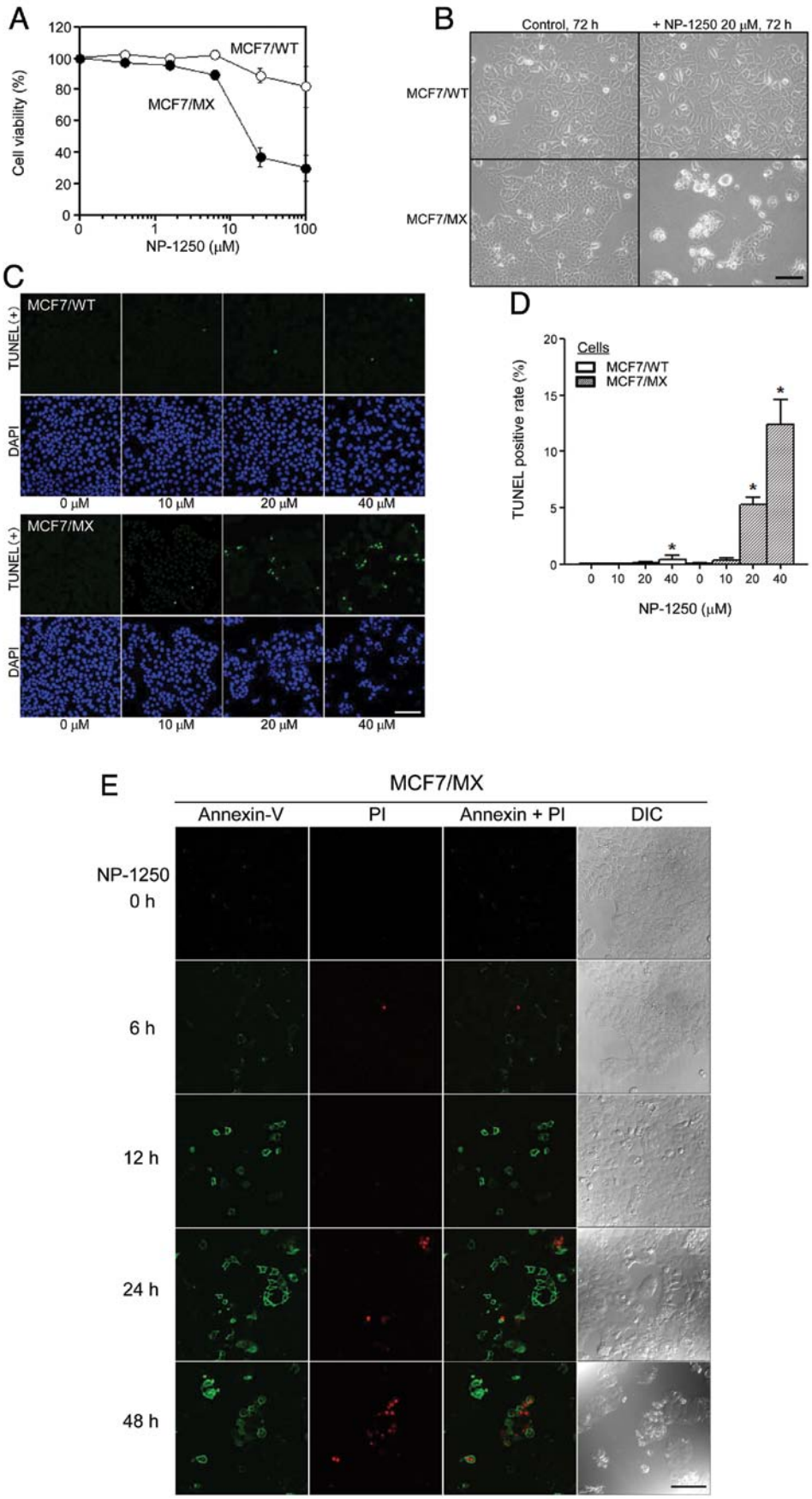

Figure 3. Effect of NP-1250 on cell growth and apoptosis of MCF7/WT and MCF7/MX cells. (A) Dose response effects of NP-1250 on cell viability. Data points, means; bars, SD (n=3). (B) Cell morphological changes after a 72-h incubation with 20 μM of NP-1250. Scale bar, 200 μm. (C) TUNEL staining after a 48-h incubation with NP-1250. Scale bar, 100 μm. (D) TUNEL-positive ratio calculated as described. Columns, means; bars, SD (*P<0.01). (E) MCF7/MX cells incubated with 20 μM of NP-1250 were examined for Annexin V/PI staining. Cells undergoing early stage apoptosis were visualized by binding of (fluoresein-conjugated) Annexin V to translocated phosphatidylserine (green). Cells with a ruptured plasma membrane in the process of cell death were visualized by binding of propidium iodide (PI) to cellular nucleic acid (red). Scale bar, 100 μm.

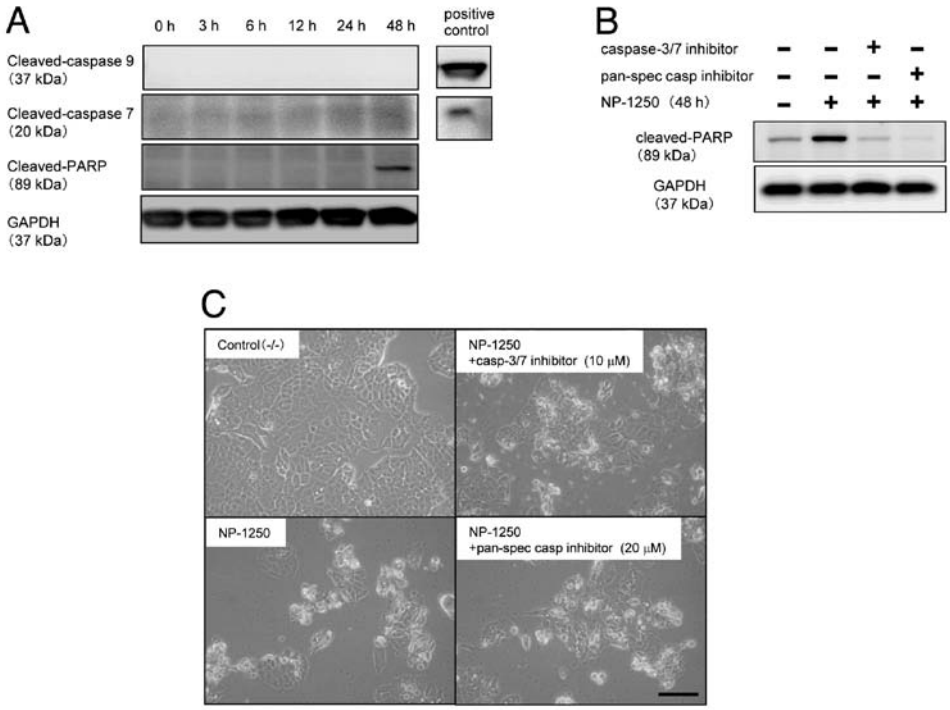

Figure 4. NP-1250-induced apoptosis of MCF7/MX cells involves caspase activation but is 'caspase-independent'. (A) Induction of the cleavage of PARP, a substrate for caspase-3/7, in NP-1250-treated MCF7/MX cells. GAPDH was used as a loading control. Positive controls: cleaved-caspase-9, protein lysate of HeLa cells treated with 1 mM staurosporine for 6 h; cleaved-caspase-7, protein lysates of MCF7 cells treated with 1 mM staurosporine for 3 h. Pretreatment with caspase-3/7 inhibitor or pan-specific inhibitor led to significant reduction in PARP cleavage (B) but did not block NP-1250-induced apoptotic cell death (C). Scale bar, 100 μm.

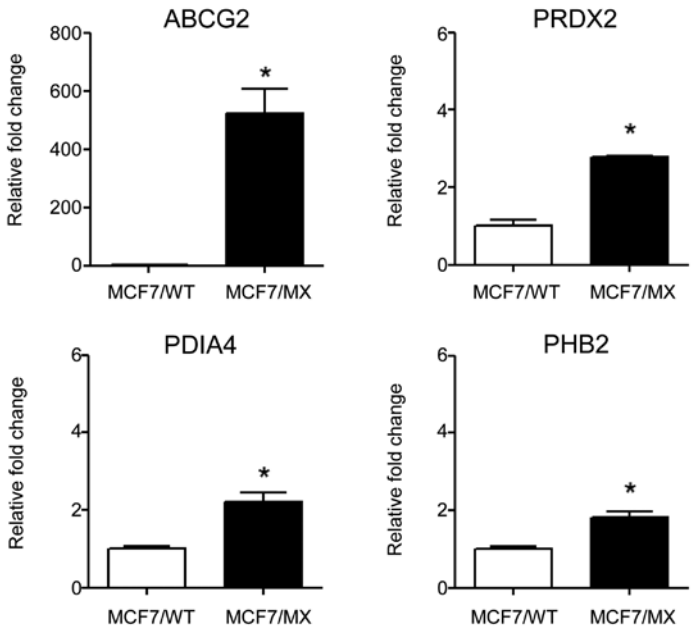

Figure 5. Proteins whose mRNAs were elevated in MCF7/MX cells. ABCG2, ATP-binding cassette, subfamily G, member 2. PRDX2, peroxiredoxin-2. PDIA4, protein disulfide-isomerase A4. PHB2, prohibitin-2. Columns, means; bars, SD (n=3; *P<0.01).

inhibit the transcriptional activity of the ER (16). While PHB2 has been implicated in a previously uncharacterized pathway of multidrug resistance in *Caenorhabditis elegans* (17), Keenan *et al* found that PHB2 was inversely correlated with resistance in a squamous lung cancer cell line (14). PRDX2 has been previously known as a natural killer-enhancing factor B (18) and is induced by various oxidative stimuli. It plays an important protective role against oxidative radical damage by reactive oxygen and nitrogen species (19). Its expression is correlated with resistance to apoptosis induced by radiation

Table II. The candidate target proteins of NP-1250 identified by mass spectrometry.

No.	Prot_acc[a]	Identified protein[a]	Prot_pI[b]	Prot_mass[b]	Prot_score[c]
1	PRDX2_HUMAN	Peroxiredoxin-2	5.66	22,091	533
2	RL9_HUMAN	60S ribosomal protein L9	9.96	21,992	274
3	RL18_HUMAN	60S ribosomal protein L18	11.73	21,763	232
4	RAB7A_HUMAN	Ras-related protein Rab-7a	6.40	23,830	191
5	RS5_HUMAN	40S ribosomal protein S5	9.73	23,075	256
6	LGUL_HUMAN	Lactoylglutathione lyase	5.12	21,048	145
7	RHOA_HUMAN	Transforming protein RhoA	5.83	22,180	184
8	COMD3_HUMAN	COMM domain-containing protein 3	5.63	22,421	118
9	RAB10_HUMAN	Ras-related protein Rab-10	8.59	22,811	150
10	PRDX1_HUMAN	Peroxiredoxin-1	8.27	22,380	146
11	GLTP_HUMAN	Glycolipid transfer protein	6.90	24,048	112
12	TAGL2_HUMAN	Transgelin-2	8.41	22,590	648
13	PSB5_HUMAN	Proteasome subunit β type-5	6.43	28,675	420
14	PEBP1_HUMAN	Phosphatidylethanolamine-binding protein 1	7.01	21,186	366
15	RS7_HUMAN	40S ribosomal protein S7	10.09	22,113	248
16	RS9_HUMAN	40S ribosomal protein S9	10.66	22,649	262
17	GGCT_HUMAN	γ-glutamylcyclotransferase	5.07	21,278	185
18	GNA1_HUMAN	Glucosamine 6-phosphate N-acetyltransferase	8.17	21,162	147
19	DCTP1_HUMAN	dCTP pyrophosphatase 1	4.93	18,811	105
20	RCL_HUMAN	Deoxyribonucleoside 5'-monophosphate N-glycosidase	4.97	19,239	110
21	DCD_HUMAN	Dermcidin	6.08	11,419	100
22	LDHA_HUMAN	L-lactate dehydrogenase A chain	8.44	37,021	566
23	PCNA_HUMAN	Proliferating cell nuclear antigen	4.57	29,177	346
24	RL5_HUMAN	60S ribosomal protein L5	9.73	34,625	333
25	IPYR_HUMAN	Inorganic pyrophosphatase	5.54	33,207	284
26	RL6_HUMAN	60S ribosomal protein L6	10.59	32,779	289
27	RA1L3_HUMAN	Putative heterogeneous nuclear ribonucleoprotein A1-like 3	9.23	34,415	180
28	OTUB1_HUMAN	Ubiquitin thioesterase OTUB1	4.85	31,549	176
29	CHIP_HUMAN	E3 ubiquitin-protein ligase CHIP	5.61	35,403	110
30	AN32E_HUMAN	Acidic leucine-rich nuclear phosphoprotein 32 family member E	3.77	30,958	106
31	PP4C_HUMAN	Serine/threonine-protein phosphatase 4 catalytic subunit	4.91	35,768	115
32	NACA_HUMAN	Nascent polypeptide-associated complex subunit α	4.52	23,370	117
33	PHB2_HUMAN	Prohibitin-2	9.83	33,276	489
34	VDAC2_HUMAN	Voltage-dependent anion-selective channel protein 2	7.49	32,186	319
35	ROA1_HUMAN	Heterogeneous nuclear ribonucleoprotein A1	9.17	38,865	238
36	P5CR1_HUMAN	Pyrroline-5-carboxylate reductase 1, mitochondrial	7.18	33,624	356
37	EFTS_HUMAN	Elongation factor Ts, mitochondrial	8.62	35,794	157
38	ELAV1_HUMAN	ELAV-like protein 1	9.23	36,282	143
39	SFXN1_HUMAN	Sideroflexin-1	9.22	35,952	108
40	PDIA4_HUMAN	Protein disulfide-isomerase A4	4.96	73,313	1,623
41	HNRPM_HUMAN	Heterogeneous nuclear ribonucleoprotein M	8.84	77,819	566
42	ECHA_HUMAN	Trifunctional enzyme subunit α, mitochondrial	9.16	83,870	331
43	ABCG2_HUMAN	ATP-binding cassette sub-family G member 2	8.91	73,120	192
44	GPDM_HUMAN	Glycerol-3-phosphate dehydrogenase, mitochondrial	7.57	81,441	262
45	TRAP1_HUMAN	Heat shock protein 75 kDa, mitochondrial	8.30	80,415	117
46	GRP78_HUMAN	Glucose-regulated protein 78 kDa	5.07	72,431	248

[a]Proteins were derived from Swiss-Prot and the National Center for Biotechnology Information non-redundant databases. [b]Theoretical pI and molecular weight obtained from Swiss-Prot. [c]MASCOT score for the identified proteins based on the peptide ion score.

therapy or anticancer drugs (20), highlighting the potential clinical importance of PRDX2 in chemotherapy resistance in cancer. However, the association of PRDX2 and MCF7/MX cells has not been previously reported. Thus further studies, such as knockdown experiments, are warranted.

In the present study, NP-1250 showed no cytostatic effect on other MDR cancer cell lines. However, it may be effective against specific tumors that are clinically similar to MCF7/MX cells and there is still a possibility that it may lead to the identification of new therapeutic molecules for MDR cancers.

Acknowledgements

We thank Dr Takaichi Hamano (Nippon Chemiphar Co., Ltd.) for the helpful discussions. This study was supported by a Grant-in-Aid for Cancer Research and Grants-in Aid for Scientific Research from the Ministry of Education, Culture, Sports, Science and Technology of Japan, and the Ministry of Health, Labor and Welfare of Japan.

References

1. Scheffer GL, Maliepaard M, Pijnenborg AC, *et al*: Breast cancer resistance protein is localized at the plasma membrane in mitoxantrone- and topotecan-resistant cell lines. Cancer Res 60: 2589-2593, 2000.
2. Kuo MT: Roles of multidrug resistance genes in breast cancer chemoresistance. Adv Exp Med Biol 608: 23-30, 2007.
3. Guo X, Ma N, Wang J, Song J, Bu X, Cheng Y, *et al*: Increased p38-MAPK is responsible for chemotherapy resistance in human gastric cancer cells. BMC Cancer 8: 375, 2008.
4. Honma K, Iwao-Koizumi K, Takeshita F, Yamamoto Y, Yoshida T, Nishio K, *et al*: RPN2 gene confers docetaxel resistance in breast cancer. Nat Med 14: 939-948, 2008.
5. Katoh SY, Ueno M and Takakura N: Involvement of MDR1 function in proliferation of tumour cells. J Biochem 143: 517-524, 2008.
6. Chen Z, Liu F, Ren Q, Zhao Q, Ren H, Lu S, *et al*: Suppression of ABCG2 inhibits cancer cell proliferation. Int J Cancer 126: 841-851, 2010.
7. Nakagawa M, Schneider E, Dixon KH, Horton J, Kelley K, Morrow C and Cowan KH: Reduced intracellular drug accumulation in the absence of P-Glycoprotein (mdr1) overexpression in mitoxantrone-resistant human MCF-7 breast cancer cells. Cancer Res 52: 6175-6181, 1992.
8. Wakabayashi K, Nakagawa H, Adachi T, Kii I, Kobatake E, Kudo A and Ishikawa T: Identification of cysteine residues critically involved in homodimer formation and protein expression of human ATP-binding cassette transporter ABCG2: a new approach using the flp recombinase system. J Exp Ther Oncol 5: 205-222, 2006.
9. Saito H, Hirano H, Nakagawa H, Fukami T, Oosumi K, Murakami K, *et al*: A new strategy of high-speed screening and quantitative structure-activity relationship analysis to evaluate human ATP-binding cassette transporter ABCG2-drug interactions. J Pharmacol Exp Ther 317: 1114-1124, 2006.
10. Wang T, Kajino K, Abe M, Tan K, Maruo M, Sun G, *et al*: Suppression of cell death by the secretory form of N-terminal ERC/mesothelin. Int J Mol Med 26: 185-191, 2010.
11. Fujimura T, Shinohara Y, Tissot B, Pang PC, Kurogochi M, Saito S, *et al*: Glycosylation status of haptoglobin in sera of patients with prostate cancer vs. benign prostate disease of normal subjects. Int J Cancer 122: 39-49, 2008.
12. Janicke RU, Sprengart ML, Wati MR and Porter AG: Caspase-3 is required for DNA fragmentation and morphological changes associated with apoptosis. J Biol Chem 273: 9357-9360, 1998.
13. Wilkinson B and Gilbert HF: Protein disulfide isomerase. Biochim Biophys Acta 1699: 35-44, 2004.
14. Keenan J, Murphy L, Henry M, Meleady P and Clynes M: Proteomic analysis of multidrug-resistance mechanisms in adriamycin-resistant variants of DLKP, a squamous lung cancer cell line. Proteomics 9: 1556-1566, 2009.
15. Liu Y, Liu H, Han B and Zhang JT: Identification of 14-3-3sigma as a contributor to drug resistance in human breast cancer cells using functional proteomic analysis. Cancer Res 66: 3248-3255, 2006.
16. Montano MM, Ekena K, Delage-Mourroux R, Chang W, Martini P and Katzenellenbogen BS: An estrogen receptor-selective coregulator that potentiates the effectiveness of antiestrogens and represses the activity of estrogens. Proc Natl Acad Sci USA 96: 6947-6952, 1999.
17. Zubovych I, Doundoulakis T, Harran PG and Roth MG: A missense mutation in *Caenorhabditis elegans* prohibitin 2 confers an atypical multidrug resistance. Proc Natl Acad Sci USA 103: 15523-15528, 2006.
18. Shau H and Kim A: Identification of natural killer enhancing factor as a major antioxidant in human red blood cells. Biochem Biophys Res Commun 199: 83-88, 1994.
19. Kowaltowski AJ, Netto LE and Vercesi AE: The thiol-specific antioxidant enzyme prevents mitochondrial permeability transition evidence for the participation of reactive oxygen species in this mechanism. J Biol Chem 273: 12766-12769, 1998.
20. Chung YM, Yoo YD, Park JK, Kim YT and Kim HJ: Increased expression of peroxiredoxin II confers resistance to cisplatin. Anticancer Res 21: 1129-1133, 2001.